A Physical Interpretation for Anomalous Source Spectra with a Deficit at Intermediate Frequencies

Yongfei Wang[1,2]; Steven M. Day[1]; Peter M. Shearer[2]

[1]Department of Geological Sciences, San Diego State University, San Diego, USA
[2]Institute of Geophysics and Planetary Physics, Scripps Institution of Oceanography, University of California, San Diego, San Diego, USA

Contact: Yongfei Wang (yow004@ucsd.edu)

Abstract

Many small crustal events in the northern Ibaraki prefecture and the Fukushima prefecture Hamadori area of Japan deviate systematically from the standard omega-square model, with an intermediate-frequency deficit (concavity) in the spectra and low- and high-frequency bumps in residual spectra that may reflect source complexity (Uchide and Imanishi, 2016). This anomaly may result from propagation effects (e.g., multipathing or attenuation) or source complexity (e.g., asperity or barrier models). We investigate the multipathing hypothesis by testing if the anomaly is specific to certain stations or paths, but find that the anomaly is broadly distributed over station location, azimuth, and source depth. With respect to attenuation, we find that a frequency-dependent Q model (e.g., power-law Q) can theoretically explain the spectral concavity if the falloff of inverse Q at high frequency is close to predictions of a Debye peak, but the required falloff rate (-1) is much steeper than permitted from Q studies and observations of source spectra. Thus, source effects are a more likely explanation for the anomalous spectra and we find that a composite source model (an outer big circle filled with smaller subevents) can account for the concavity in spectra. Compared with asperity models with varying stress drop, a model with appreciable acceleration/deacceleration in rupture velocity and variant subevent sizes appears a viable candidate. By simulating dynamic rupture scenarios and performing analytical derivations, we discover such a model has: (1) a high frequency decay with omega-square asymptote that is mainly controlled by outer marginal stopping phases, (2) spectral concavity that is related to the spatial density and the maximum/minimum radius of the subevents, and (3) seismic moment in this composite source is self-similarly proportional to the cube of the outer radius. Thus, based on spectra from our dynamic simulations, we can construct a physical link between stress drop and apparent corner frequency for our composite source model, similar to that described for simpler models in Madariaga (1976), Kaneko and Shearer (2014, 2015), and Wang and Day (2017). In the future, we would like to generalize a spectral model to deal with composite sources to better characterize source complexities and stress regimes.

Background

Small crustal events (in total 196 Mw3.2-4 events shallower than 20 km) in the northern Ibaraki prefecture and the Fukushima prefecture Hamadori area of Japan deviate systematically from the standard omega-square model, with an intermediate-frequency deficit (concavity) in the spectra (Uchide and Imanishi, 2016).

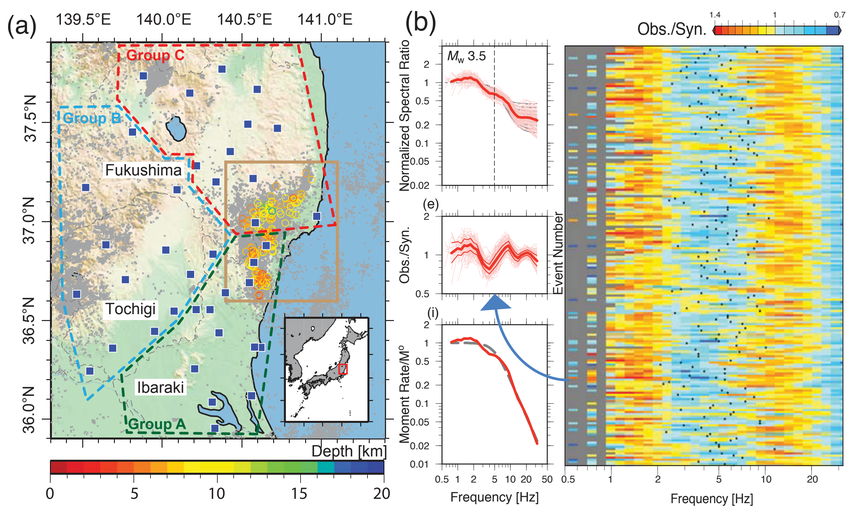

Figure 1. a) the location of the seismicity and stations in this study, b) examples of anomalous P wave spectra

Key question:
what physical mechanisms can account for it ?

Intermediate-frequency deficit in spectra

Path Effects
Multi-pathing (localized high/low velocity anomaly)
Frequency-dependent attenuation
...

Source Effects
Nonuniform stress drop (asperities)
Nonuniform rupture velocity (barriers)
...

Path Effects

1. We first study multi-pathing effects (multiple arrivals of P wave caused by localized high/low velocity anomalies). If the multi-pathing is causing the intermediate-frequency deficit, the spectra deficit (spectral concavity) should observe a spatial pattern of path-dependency (azimuthal- or depth-dependent anomalies related to lateral or vertical velocity structure). To quantify the deficit level, we define the concavity as a dimensionless quantity: the mean ratio between upper envelope (S_2) and observed (S_1) residual spectra (obs/syn) within the frequency band constrained by the two peaks (f_1 and f_2) of the observed residual spectra, and then multiplied by the ratio of f_2 and f_1, as indicated in Figure 2.

$$ccv = \frac{\int_{f_1}^{f_2} \frac{S_2(f)}{S_1(f)}\, df}{f_2 - f_1} \frac{f_2 - f_1}{f_1}$$

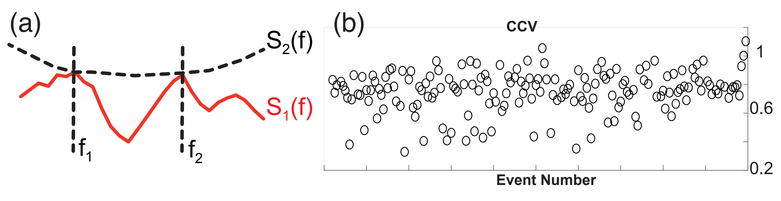

Figure 2. (a) Schematic figure to show the methodology to measure concavity(CCV) (b) estimated CCV value of all 196 events in this study (average value is about 0.7)

We first divide all the stations into 3 groups based on their azimuthal angles (comparable number of stations in each group). In each group, we stack the spectra (the median of observed P wave spectral ratios multiplied by the best-fitting EGF spectra) of stations belonging to this group and then stack them over all the studied events. The 3 resultant residual spectra (stacked spectra divided by the best-fitting omega-square model) are plotted in Figure 3a. In contrast, we stack the spectra of the events within each depth bin (8 bins in total from 4 to 11 km) and then stack them over all stations. Residual spectra in this scenario are plotted in Figure 3b. As seen in these two figures, no systematic dependency of concavity on azimuth and depth can be found. Stacking was also applied simultaneously to station groups and focal depth bins, and to different focal depth bins with respect to one station (Figure 3c and 3d), and in each case showed no strong dependency.

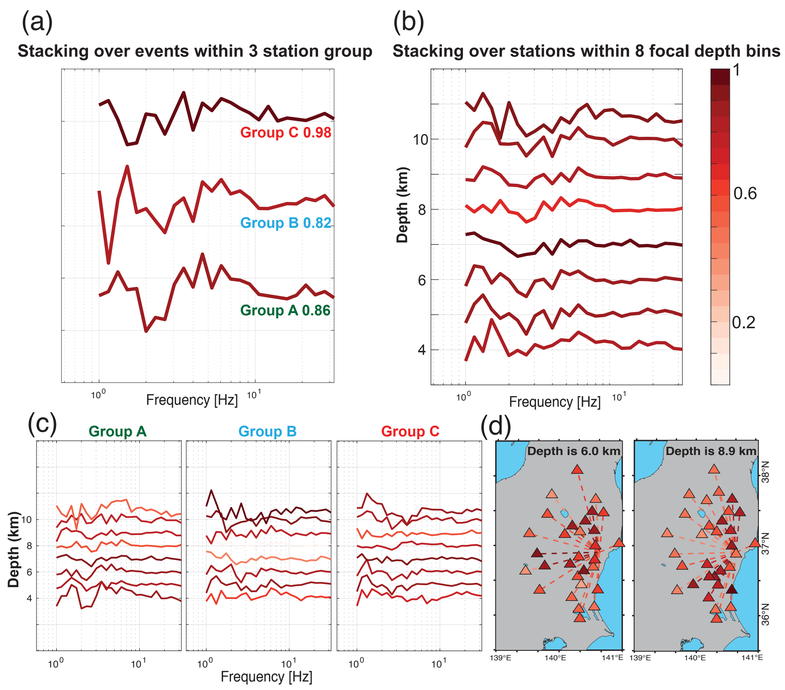

Figure 3. (a) Residual spectra of 3 different station groups. (b) Residual spectra of focal depth bins from 4 to 11 km. (c) Residual spectra of focal depth bins in different station groups. (d) Concavity index value of each station at two example focal depth bins.

2. Next we investigate if a frequency-dependent attenuation model can contribute to the anomalous spectra (assuming that the EGF deconvolution may not fully correct for attenuation). In Figure 4, we try constant Q, the absorption band model, the standard linear solid (contains a Debye Peak) and the power-law model. Some of them can mathematically explain the concavity if the falloff of inverse Q at high frequency is close to what a Debye peak predicts (falloff is ~ -1) but this is much steeper than permitted from Q studies and observations of source spectra.

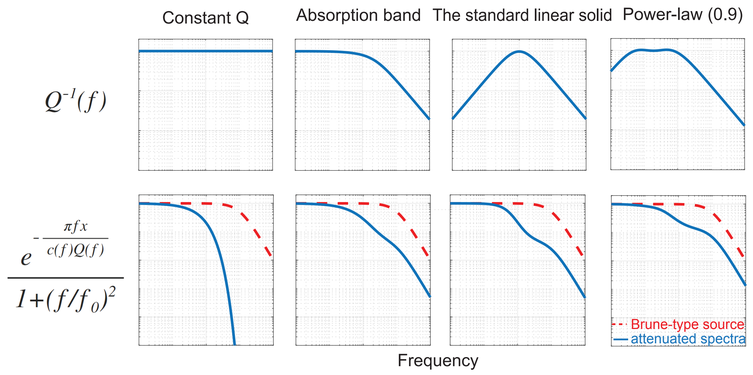

Figure 4. Q inverse of attenuation models: constant Q, absorption band model, the standard linear solid and the power-law model and the comparison between the spectra of a Brune-type source and attenuated spectra by these models.

Source Effects

3. We first explore 2 kinds of simple deviations from classic crack models: nonuniform stress drop (asperity) and variable rupture velocity (barrier). Theoretically, both models can modify high- and low- frequency seismic radiation and provide a chance to produce an intermediate-frequency deficit in spectra. Here we generate 4 models as seen in Figure 5, the synthetic far-field spectra of variable rupture velocities show a greater potential (than nonuniform stress drop models) to reproduce the concavity discovered in our observed datasets. Of course, in reality, these two complexities are possibly coupled (e.g., an overstressed asperity can not only undertake a larger stress drop but also spontaneously accelerate the rupture). Therefore, variable rupture velocity is favored in generating the spectral intermediate-frequency deficit.

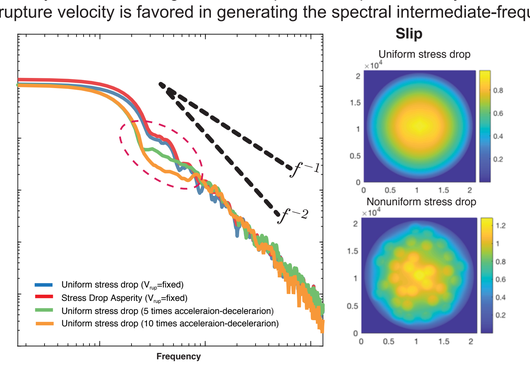

Figure 5. Displacement spectra of 4 models: classic crack (uniform (preset) stress drop), nonuniform stress drop with fixed rupture velocity and 2 models with uniform stress drop and variable rupture velocity.

4. But the rupture velocity is very hard to constrain, especially for small earthquakes. An alternative source (which contains the variation of rupture velocity when across the edges of subevents) model should be able to generate both traditional (Brune type) and anomalous (concave) source spectra, thus this alternative will serve as a generalized instead of special source model. Thus, a composite source model in which the sizes of subevents obey a self-similar power-law distribution (fractal dimension D=2) can produce an event with stress drop independent of seismic moment, an omega-square high-frequency falloff and *b* value of 1 (Frankel, 1991; Zeng et al, 1994). So we implement a fractal dimension source model (Figure 6) and simulate the far-field spectra of this model (Figure 7).

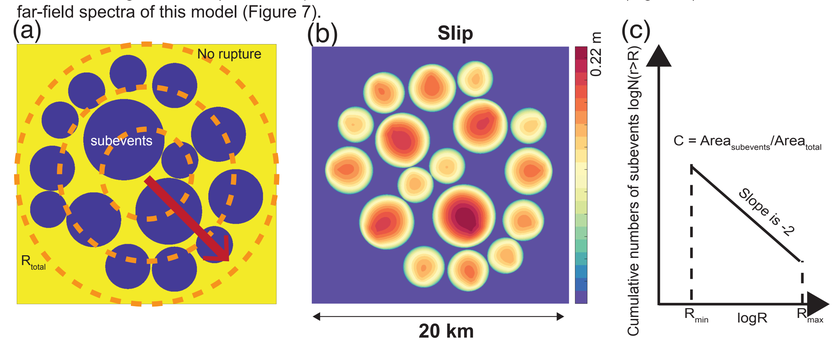

Figure 6. (a) schematic fractal composite source model (blue circles are subevents beyond which no rupture is allowed). Subevents are sequentially triggered from the center of outer circle (R_{total}). (b) An example of a slip distribution caused by a composite source (a). (c) shows in this model the cumulative number of subevents follows a power law of the radius and the parameters required to describe a fractal composite source. R_{max} and R_{min} are the maximum and minimum radii of the subevents. C is the spatial rupture density defined as the ratio between the area of subevents and the total area within the outer circle (R_{total}).

Based on the previous study (Frankel, 1994), we analytically derive the low and high-frequency asymptotic level of far-field spectrum:

$$\Omega_L^{comp} = E_1 \frac{16}{7} R_{total}^3 \Delta\sigma \qquad E_1 = \frac{c(R_{max}-R_{min})}{R_{total}\ln(R_{max}/R_{min})}$$

$$\Omega_H^{comp} = E_2 (C_s \beta / f)^2 \frac{16}{7} R_{total} \Delta\sigma \qquad E_2 = \sqrt{c}$$

From the equations above, the high-frequency asymptotic level is only dependent on the spatial rupture density and R_{total}, which can be confirmed by our dynamic fractal source model (Figure 7a). In addition, the observed intermediate-frequency deficit is reproduced in our dynamic fractal models and the concavity relies on the proximity of R_{max} to R_{min}. We determine a corner frequency by only fitting the low- and high- frequency asymptotic levels, ignoring the intermediate-frequency deficit. The corner frequencies, estimated from our dynamic fractal models with as largely varying values of parameters of C, R_{total}, R_{max} and R_{min} as possible, given computational limitations (642 in total), are still close to self-similarity ($f_c \sim M_0^{-1/3}$) (Figure 7b)

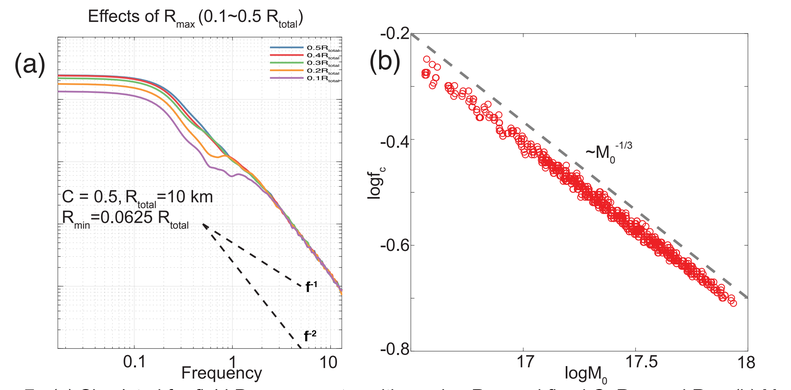

Figure 7. (a) Simulated far-field P-wave spectra with varying R_{max} and fixed C, R_{total} and R_{min}. (b) Measured corner frequencies by only fitting low and high-frequency asymptotic level in 642 dynamic fractal models (R_{total}(4.5 km ~ 10 km), R_{max} ($0.2R_{total}$~$0.45R_{total}$), C(0.3~0.6) and R_{min} ($0.15R_{total}$).

Correspondingly, we measure corner frequencies of observed spectra by only low- and high- frequency fitting ignoring the intermediate-frequency concavity (Figure 8). The preliminarily estimated values of corner frequencies show non-cuberoot dependency on seismic moment.

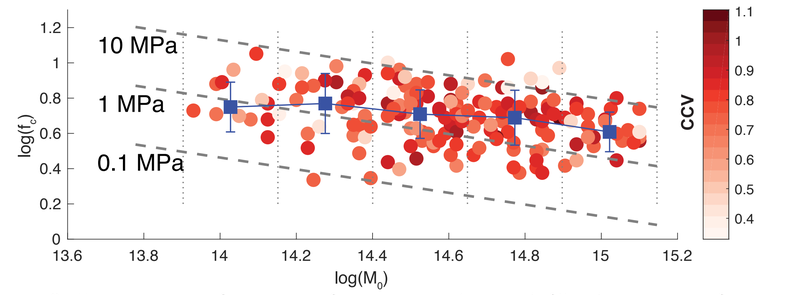

Figure 8. Measured corner frequencies of observed spectra by only fitting low- and high- frequency asymptotic level. The slope (blue line) in log-log scale is -0.15.

Summary

1.Multi-pathing and attenuation can not completely account for the intermediate-frequency deficit in observed spectra
2. Variable rupture velocity is required to reproduce the spectral concavity
3. Spectral concavity in dynamic composite source model is related to the maximum/minimum radius of the subevents
4. Model corner frequency measured by only fitting the low- and high- frequency asymptotic level is self-similarly inversely proportional to the cube root of the seismic moment
5. Similar measurements apply to observed spectra and the corner frequencies show non-cuberoot dependency of the seismic moments